

# Environmental control of microtubule-based bidirectional cargo-transport

Sarah Klein,<sup>1,2</sup> Cécile Appert-Rolland,<sup>1</sup> and Ludger Santen<sup>2</sup>

<sup>1</sup>Laboratory of Theoretical Physics, CNRS (UMR 8627),

University Paris-Sud Bâtiment 210, F-91405 ORSAY Cedex, France

<sup>2</sup>Fachrichtung Theoretische Physik, Universität des Saarlandes D-66123 Saarbrücken, Germany

(Dated: July 19, 2022)

Inside cells, various cargos are transported by teams of molecular motors. Intriguingly, the motors involved generally have opposite pulling directions, and the resulting cargo dynamics is a biased stochastic motion. It is an open question how the cell can control this bias. Here we develop a model which takes explicitly into account the elastic coupling of the cargo with each motor. We show that bias can be simply controlled or even reversed in a counterintuitive manner via a change in the external force exerted on the cargo or a variation of the ATP binding rate to motors. Furthermore, the superdiffusive behavior found at short time scales indicates the emergence of motor cooperation induced by cargo-mediated coupling.

PACS numbers:

## INTRODUCTION

In cells, most of the active transport processes, which are essential for cellular functions, are driven by molecular motors. These molecular motors are proteins having the ability to move preferentially in a defined direction on the polar filaments of the cytoskeleton [1]. The three most well-known molecular motors' families involved in transport are myosins, which move on actin filaments, dyneins and kinesins, which use microtubules (MT) as tracks [2]. Kinesin motors are stepping preferentially toward the growing (or plus-) end of MTs while dynein motors walk in the opposite direction.

Molecular motors can step individually or transport cargos along the cytoskeletal filaments. In order to generate forces large enough [3] to move a big cargo in the crowded environment of the cell, cargos are often transported by teams of molecular motors [4]. This is obviously beneficial if motors of the same type are attached to the cargo, since the force can be distributed between them. It enhances the processivity of the cargo and its ability to resist against forces emerging when transporting the cargo.

In many cases, however, motors that are attached to a given cargo pull in opposite preferential directions. Surprisingly, the attachment of two kinds of motors is not only observed for objects like mitochondria, which have to be spread out in the whole cell volume [5], but also for cargos which have a definite target, for example to be transported from the cell center to the membrane or *vice versa* [6].

Although the attachment of two kinds of motors should enable bidirectional transport it is expected that, due to the difference in the characteristics of the various types of motors attached to the cargo [7] and possibly in the number of attached motors, the cargo undergoes a *biased* stochastic walk if the MT network is oriented.

Depending on the given motor-cargo system and the

environment of the filaments different types of motion have been observed, which can be controlled by different mechanisms.

Some pigment cells (melanosomes) for example have the ability to switch between two states, in which the pigments are either dispersed or aggregated at one extremity of the filaments [8, 9]. The mechanisms that allow for such a transition from a non-biased to a biased motion are not yet well understood but have been related to signaling processes which regulate the activity of the attached motors [10].

Next to the regulation of the motors' activity also the cellular environment plays an important role. Recent *in vivo* experimental studies on cargos transported bidirectionally have revealed a very complex dynamical behavior. Super- as well as subdiffusive regimes of the cargos' trajectories have been identified [11–13]. Bidirectional cargo transport on MT networks has also been studied *in vitro* and enhanced diffusion was obtained as well [14]. It was also observed that a change in direction often occurs due to cellular obstacles like other cargos or the cytoskeleton itself [15]. In order to disentangle the action of different external control mechanisms on motor-cargo complexes we study their dynamics by means of a theoretical model.

The stochastic model we introduce in this work describes bidirectional cargo-motion along microtubules, which is driven by teams of kinesin and dynein motors. We will show that a variation of the ATP-hydrolysis rate changes the cargo-dynamics in a non-trivial way and can even invert the direction of the bias. A non-trivial response to the effective viscosity of the environment (representing the crowdedness of the surrounding cytoskeleton) is also obtained as a result of the complex interaction between the attached molecular motors. Additionally, we show that, as observed in several *in vivo* experiments [12, 13], super-diffusive particle motion can be observed in our model.

## MODEL

We introduce a stochastic model for the transport of a cargo by teams of molecular motors along a single microtubule. Several approaches to describe this behavior were given in the last years [7, 16–18]. In our model, which is inspired by the bidirectional cargo transport models of [7, 16],  $N_+$  and  $N_-$  motors are tightly bound to the cargo and pull it in plus- and minus-direction, respectively. Throughout the paper we shall taken  $N_+ = N_-$ . In contrast to [16] we take every single motor position  $x_i$  into account and calculate the thereby generated force  $F_i$  on the cargo. We model the tail of the molecular motors, which permanently connects the motor domain with the cargo, as a linear spring with untensioned length  $L_0$  and spring constant  $\alpha$  (FIG. 1). The motors can perform three different actions: if they are bound to the filament, which is represented as a one-dimensional lattice, they can make a step of size  $d$  or detach from the filament. Both events occur with force-dependent rates  $s(F_i)$  and  $k_d^\pm(F_i)$ , respectively. Once a motor has detached from the filament, it can reattach in the interval  $\pm L_0$  around the cargo's center of mass with a force-independent rate  $k_a$ . Due to the de-/attachment events the number of plus (minus) motors bound to the filament is in the range  $0 \leq n_+ \leq N_+$  ( $0 \leq n_- \leq N_-$ ). The resulting force on the cargo at position  $x_C(t)$  at time  $t$  is then given by the sum of all single forces applied by bound motors

$$F(x_C(t), \{x_i\}) = \sum_{i=1}^{n_+ + n_-} F_i(x_i - x_C(t)) \quad (1)$$

with  $F_i(x_i - x_C(t)) =$

$$\begin{cases} \alpha(x_i - x_C(t) + L_0), & x_i - x_C(t) < -L_0 \\ 0, & |x_i - x_C(t)| < L_0 \\ \alpha(x_i - x_C(t) - L_0), & x_i - x_C(t) > L_0 \end{cases}$$

The motor's stepping behavior depends on the surrounding ATP concentration ( $[ATP]$ ) as well as the force  $F_i$  applied to the cargo. As mentioned above, forces that are acting on the motors change their detachment and stepping rate. If the force is acting against the preferred direction the motor may slow down, stop or even invert its direction. The maximal force (in absolute value) under which a motor still walks in its preferred direction is given by  $F_S$ . We shall thus distinguish two regimes for the stepping behavior, depending whether the applied force is smaller than the stall force (regime I) or larger (regime II). In regime I (+end motors:  $0 \leq F_i < F_S$  / -end motors  $-F_S < F_i \leq 0$ ), we use a 2-state Michaelis-Menten equation [19] (see Supplementary for further information) to define the stepping rate  $s(|F_i|, [ATP])$  via

$$s(|F_i|, [ATP]) = \frac{k_{\text{cat}}(|F_i|)[ATP]}{[ATP] + \frac{k_{\text{cat}}(|F_i|)}{k_b(|F_i|)}}, \quad (2)$$

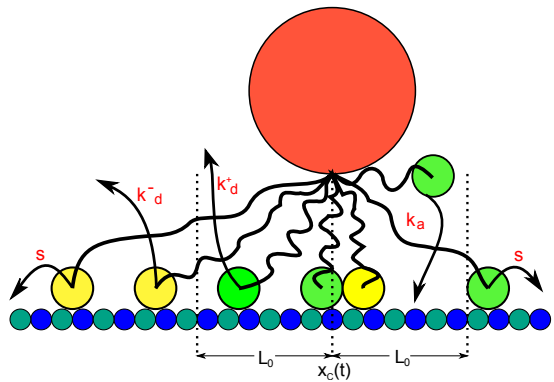


FIG. 1: Sketch of the model dynamics. The cargo (red) is pulled by two families of molecular motors (yellow and green) hopping in opposite directions on the MT.

with the catalytic-turnover rate constant  $k_{\text{cat}}(|F_i|)$  and a second-order rate constant for ATP binding  $k_b(|F_i|)$ .

In regime II (+end motors:  $F_i \geq F_S$  / -end motors  $-F_S \geq F_i$ ), the motors can walk backwards with the constant rate

$$s(F_i) = \frac{v_b}{d}, \quad (3)$$

corresponding to the backward velocity  $v_b$ , which is at least one order smaller than the force-free forward velocity. In the model we neglect any motor position exclusion on the filament since motors can walk on several lanes of the microtubule. Furthermore the MT network is very dense in many cell regions, as for example in axons where the distance between two microtubules is about 20 nm [20]. There, motors can walk on multiple microtubules around the pulled cargo.

We choose the detachment behavior according to [7]

$$k_d^+(F_i) = \begin{cases} k_d^0 \exp\left(\frac{|F_i|}{2.5f}\right) & F_i < F_S \\ k_d^0 \left(0.186 \frac{|F_i|}{f} + 1.535\right) & F_i \geq F_S \end{cases} \quad (4)$$

for kinesin and

$$k_d^-(F_i) = \begin{cases} k_d^0 \exp\left(\frac{|F_i|}{2.5f}\right) & F_i > -F_S \\ k_d^0 \left[1.5 \left(1 - \exp\left(\frac{-|F_i|}{1.97f}\right)\right)\right]^{-1} & F_i \leq -F_S \end{cases} \quad (5)$$

for dynein. We use the force-free detachment rate  $k_d^0$  and a standardization force  $f = 1$  pN which determines the force scale. Note that the behavior of both types of motors differs above stall, where we have a catch-bond like rate (decreasing with  $F_i$ ) for dynein. We propagate the system by means of Gillespie's algorithm for time-dependent rates [21], since the force exerted on each motor (and thus the rates) is time-dependent (see Supplementary for further information). The viscosity  $\eta$  of the cytoskeleton is taken into account when we solve the

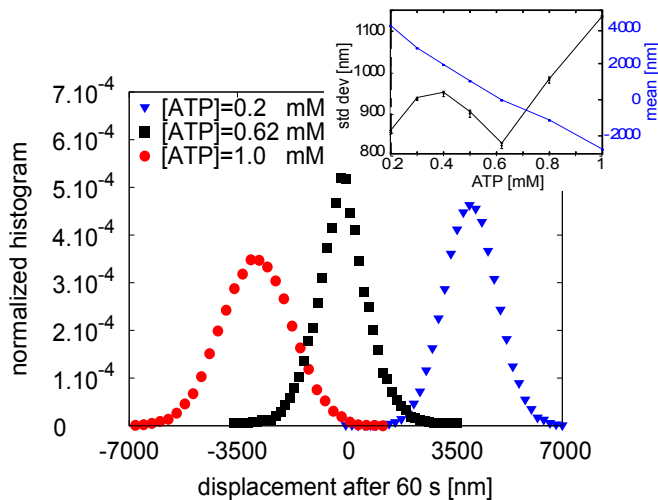


FIG. 2: Normalized histogram of the displacement after 60 s of cargo propagation. The red circles correspond to  $[ATP]=0.2$  mM, the black squares to  $[ATP]=0.62$  mM and the blue triangles to  $[ATP]=1.0$  mM. We get for the mean displacement  $\mu_{0.2} = 4028.3 \pm 1.14$  nm and the standard deviation  $\sigma_{0.2} = 855.9 \pm 1.13$  nm for  $[ATP] = 0.2$  mM,  $\mu_{1.0} = -2887.5 \pm 3.17$  nm and  $\sigma_{1.0} = 1139.9 \pm 2.59$  nm for  $[ATP] = 1.0$  mM and  $\mu_{0.62} = -27.8 \pm 14.08$  nm and  $\sigma_{0.62} = 836.9 \pm 11.5$  nm for  $[ATP] = 0.62$  mM. Obviously, the displacement changes direction from plus-end bias for stronger plus motors at low  $[ATP]$  to minus-end bias at saturating  $[ATP]$ . The inset shows the non-monotonous curve of the standard deviation of the displacement (black) against the ATP concentration while the mean displacement (blue) decreases monotonously.

equation of motion for the cargo

$$m \frac{\partial^2 x_C(t)}{\partial t^2} = -\beta \frac{\partial x_C(t)}{\partial t} + F(x_C(t), \{x_i\}), \quad (6)$$

with Stokes' law  $\beta = 6\pi\eta R$  ( $R$ : cargo radius,  $m$ : cargo's mass).

## RESULTS AND DISCUSSION

First we simulate the model in order to measure the distribution of the cargo displacement for one-minute intervals (see FIG. 2). The results, which we obtained for the model's parameters given in TABLE S1 (see Supplementary material), show that we can tune the mean velocity (or bias) of the transported cargo continuously by means of the ATP-concentration. Remarkably, the cargo *slows down with increasing* ATP-concentration until the bias vanishes (at an ATP concentration of 0.62 mM for our choice of the parameters). For larger concentrations of ATP the bias is inverted and its absolute value increases again. In contrast to scenarios based on signaling processes where a protein would up- or down-regulate only one motor species, here the inversion of the

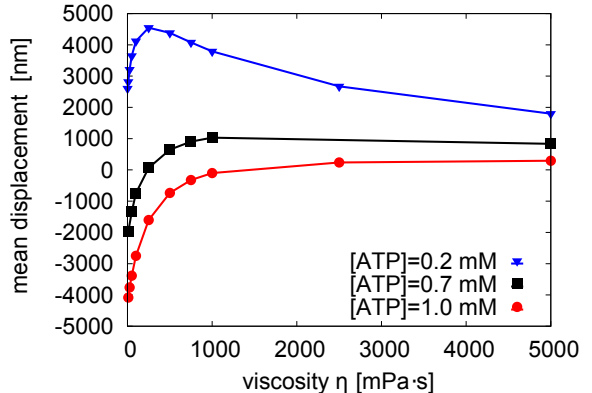


FIG. 3: Mean displacement after 60 s of cargo propagation for different cytoskeleton viscosities  $\eta$ . The red circles corresponds to the  $[ATP]=0.2$  mM, the black squares to  $[ATP]=0.7$  mM and the blue triangles to  $[ATP]=1.0$  mM. For small  $[ATP]$  the mean displacement-viscosity relation shows a non-monotonous behavior. In the case of  $[ATP]=0.7$  mM we observe a change in direction with increasing viscosity.

bias results from the difference in the  $[ATP]$  dependence of both motors activities. This result is of relevance for the search of signaling processes in cells: An inversion of the cargo's bias does not necessarily imply that only one motor species is up or down regulated, since already the response to the effective ATP-concentration is motor specific. We also notice that an unbiased motion of the cargo can only be obtained in a rather narrow interval of ATP-concentration.

The step rate of the motors does not only depend on the ATP concentration but also on the force which is applied to the motor. The external force applied to the moving cargo can be parametrized via the viscosity of the environment. In FIG. 3 we show the dependence of the mean displacement on the viscosity (for different ATP concentrations). We observe a non-trivial dependence of the bias on the viscosity. Counterintuitively, the absolute value of the bias can increase with increasing viscosity. For intermediate ATP concentrations (see, e.g., 0.7 mM in FIG. 3) one observes that the cargo is changing its direction with increasing viscosity. This effect can be used in order to leave crowded areas in the cellular environment, which correspond to high effective viscosities, and enhance thereby the efficiency of the motor-driven transport. Here we find the bias-inversion regime for a limited range of  $[ATP]$ . Depending on the cargo and the transportation task to be fulfilled it could be more favorable to be in this bias-inversion regime or in a regime of strong bias. Evolution could have selected the regime by adjusting some other parameters like the motors concentration or an asymmetry in the motor properties. Indeed,

a change in  $N_+$ ,  $N_-$  modifies the values of the external control parameters at which we observe the reversal of the bias.

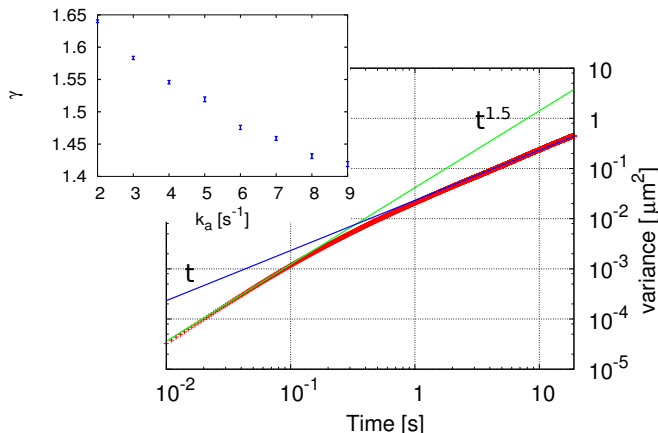


FIG. 4: Variance of the numerically generated trajectories with  $[ATP]=1$  mM. One observes at  $0.5$  s a crossover from enhanced diffusion going with  $t^\gamma$ ,  $\gamma = 1.5$  (green line) to normal diffusion proportional to  $t$  with a diffusion coefficient  $D = 0.04\mu\text{m}^2\text{s}^{-1}$  (blue line). The inset shows how the exponent varies with the attachment rate  $k_a$ .

The cargo-mediated coupling of the engaged motors induces a time-correlated motion of the cargo. These correlations lead to non-gaussian displacement distributions of the cargo at short finite time intervals (see FIG. 2). The range of the correlations can be estimated from the functional behavior of the cargo's variance. Our simulation results show the transition from enhanced diffusion at short times to normal diffusion. For the set of parameters of TABLE S1 (see Supplementary material) we observe that the variance is growing as  $t^{3/2}$  at short time scales. Thus, our model generates a superdiffusive behavior which indicates cooperation between motors induced by cargo-mediated coupling. Our results also show that the exponent is not universal (inset FIG. 4). By varying the attachment rate, which depends strongly on the cellular environment, we have been able to observe exponents that range from 1.4 to 1.6.

Asymptotically we observe purely (biased or unbiased) diffusive behavior. This asymptotic diffusive regime is generic for our model as long as we assume cargo motion on a single filament. By contrast, on a branched microtubule network the asymptotic behavior may be influenced by the structure of the network as shown in case of the microtubule-network of giant fibroblast [12], where sub-diffusive behavior has been observed.

## CONCLUSION

In this work we study the effect of environmental features on cargos transported by teams of motors.

We find that trajectories of such motor-cargo complexes exhibit different dynamic regimes. Generically one observes biased motion of the cargo, since the activity of dynein and kinesin motors can only be balanced in a very narrow interval of the external control parameters (here viscosity and ATP-concentration). The mechanical coupling of the motors induces time-correlated cargo trajectories. In the comoving frame, the correlations lead to super-diffusive behavior at short times. The exponents which describe the time evolution of the variance at short times, as well as the time at which one observes the transition to gaussian displacement distributions are parameter-dependent. For typical parameter combinations the crossover to diffusion takes place at time intervals of the order of one second.

Naively one would expect faster cargo transport for higher concentrations of ATP and lower viscosities. In this work we show that this is not the case. The response to both environmental parameters is non-monotonous. Counterintuitively, the cargo may accelerate with increasing viscosity for a given parameter-range. We also find an unexpected response of the cargo dynamics to variation of the ATP concentration. We not only observe a change of the bias but also a non-monotonous dependence of the width of the displacement distribution on the ATP concentration. The recent progress in dynein motility assays allows now to test our predictions *in vitro*. The realization of such *in vitro* assays would allow to study the mechanic coupling of molecular motors via the cargo in a much simpler environment as in the living cell. *In vivo* we do not expect relevant variations of ATP concentration. However, the ATP hydrolysis could be locally regulated at the level of motors.

In crowded areas of the cell, interactions between different cargos as well as between cargo and filament may apply forces on the molecular motors. Our model results show that, since kinesin and dynein motors respond differently to external forces, this may lead to an inversion of the cargo's bias, even if no distinct control mechanism is applied. The ability of the cargo to change its direction in a crowded environment, i.e. an environment of higher effective viscosity, may give an argument why the transport of cargo by oppositely directed motors can be beneficial for the cell.

This work was supported by the Deutsche Forschungsgemeinschaft (DFG) within the collaborative research center SFB 1027 and the research training group GRK 1276.

- 
- [1] B. Alberts, A. Johnson, J. Lewis, M. Raff, K. Roberts, and P. Walter, *Molecular biology of the cell* (Garland Science Taylor & Francis Group, 2002), 4th ed., ISBN 0815332181.
  - [2] R. Mallik and S. P. Gross, *Current Biology* **14**, R971

- (2004).
- [3] D. Chowdhury, *Physics Reports* **529**, 1 (2013).
  - [4] C. Kural, H. Kim, S. Syed, G. Goshima, V. I. Gelfand, and P. R. Selvin, *Science* **308**, 1469 (2005),
  - [5] P. J. Hollenbeck and W. M. Saxton, *Journal of cell science* **118**, 5411 (2005).
  - [6] M. A. Welte, *Current Biology* **14**, R525 (2004),
  - [7] A. Kunwar, S. K. Tripathy, J. Xu, M. K. Mattson, P. Anand, R. Sigua, M. Vershinin, R. J. McKenney, C. C. Yu, A. Mogilner, et al., *Proceedings of the National Academy of Sciences* **108**, 18960 (2011),
  - [8] S. P. Gross, M. C. Tuma, S. W. Deacon, A. S. Serpinskaya, A. R. Reilein, and V. I. Gelfand, *The Journal of Cell Biology* **156**, 855 (2002),
  - [9] A. A. Nascimento, J. T. Roland, and V. I. Gelfand, *Annual Review of Cell and Developmental Biology* **19**, 469 (2003).
  - [10] H. Nilsson Sköld, S. Aspengren, and M. Wallin, *Pigment cell & melanoma research* **26**, 29 (2013).
  - [11] I. M. Kulić, A. E. Brown, H. Kim, C. Kural, B. Blehm, P. R. Selvin, P. C. Nelson, and V. I. Gelfand, *Proceedings of the National Academy of Sciences* **105**, 10011 (2008).
  - [12] A. Caspi, R. Granek, and M. Elbaum, *Physical Review E* **66**, 011916 (2002).
  - [13] D. Robert, T.-H. Nguyen, F. Gallet, and C. Wilhelm, *PloS one* **5**, e10046 (2010).
  - [14] H. Salman, Y. Gil, R. Granek, and M. Elbaum, *Chemical physics* **284**, 389 (2002).
  - [15] L. Bruno, M. M. Echarte, and V. Levi, *Cell biochemistry and biophysics* **52**, 191 (2008).
  - [16] M. J. I. Müller, S. Klumpp, and R. Lipowsky, *Proceedings of the National Academy of Sciences* **105**, 4609 (2008),
  - [17] F. Berger, C. Keller, S. Klumpp, and R. Lipowsky, *Physical Review Letters* **108**, (2012)
  - [18] Y. Zhang, *Physical Review E - Statistical, Nonlinear, and Soft Matter Physics* **87** (2013),
  - [19] M. J. Schnitzer, K. Visscher, and S. M. Block, *Nature Cell Biology* **2**, 718 (2000).
  - [20] N. Hirokawa, Y. Noda, and Y. Okada, *Current Opinion in Cell Biology* **10**, 60 (1998),
  - [21] D. T. Gillespie, *Journal of Computational Physics* **28**, 395 (1978),

## SUPPLEMENTARY

### Cargo dynamics

Motors undergo stochastic dynamics with discrete transitions (stepwise motion, de-/attachment). By contrast, the cargo moves continuously according to a deterministic equation of motion

$$m \frac{\partial^2 x_C(t)}{\partial t^2} = -\beta \frac{\partial x_C(t)}{\partial t} + \sum_{i=1}^{n_+ + n_-} F_i(x_i - x_C(t)), \quad (\text{S1})$$

where we assume Stoke's frictional coefficient  $\beta = 6\pi\eta R$ . Equation (S1) describes the cargo motion in a viscous medium under the influence of a harmonic potential of the springs. We can generalize this equation by adding other forces like a stochastic force due to thermal noise. The force  $-F_i$  applied to each motor depends continuously on time  $t$  via the cargo position  $x_C(t)$  and thus the motor rates for stepping and detachment are time-dependent. Note that the number of tensioned springs changes, if the distance between a motor and the cargo falls below or exceeds  $L_0$ . Therefore, between two motor events, we have to solve eq. (S1) piecewise on segments with a constant number of tensioned springs. We split the the sum of forces in eq. (S1) in a constant part  $\delta$  and a part proportional to the cargo's position  $x_C(t)$

$$m \frac{\partial^2 x_C(t)}{\partial t^2} = -\beta \frac{\partial x_C(t)}{\partial t} - \epsilon x_C(t) + \delta, \quad (\text{S2})$$

where

$$\epsilon = \sum_{i=1}^{n_+ + n_-} \begin{cases} \alpha & |x_i - x_C(t)| > L_0 \\ 0 & \text{else} \end{cases} \quad (\text{S3})$$

corresponding to an effective spring constant and

$$\delta = \sum_{i=1}^{n_+ + n_-} \begin{cases} \alpha(x_i - L_0), & x_i - x_C(t) < -L_0 \\ 0, & |x_i - x_C(t)| < L_0 \\ \alpha(x_i + L_0), & x_i - x_C(t) > L_0 \end{cases}$$

which corresponds to the effective force due to the (fixed) positions of motors. The solution of eq. (S2) is

$$x_C(t) = \frac{\frac{\delta\lambda^+}{\epsilon} + \lambda^+ x_0 - v_0}{\lambda^+ - \lambda^-} \exp(\lambda^- t) + \frac{v_0 - \frac{\delta\lambda^-}{\epsilon} - \lambda^- x_0}{\lambda^+ - \lambda^-} \exp(\lambda^+ t) - \frac{\delta}{\epsilon} \quad (\text{S4})$$

with

$$\lambda^\pm = -\frac{\beta}{2m} \pm \sqrt{\left(\frac{\beta}{2m}\right)^2 - \frac{\epsilon}{m}}. \quad (\text{S5})$$

To guarantee that the cargo moves in an overdamped environment we can make a worst-case estimate for the viscosity as

$$\eta \geq \frac{\sqrt{(N_+ + N_-)\alpha m}}{3\pi R},$$

since then

$$\left(\frac{\beta}{2m}\right)^2 - \frac{\epsilon}{m} > 0 \quad (\text{S6})$$

holds and consequently the solution of eq. (S4) is an exponentially decaying function. With our chosen parameter for the cargo radius  $R$  and mass  $m$  this threshold is at  $\eta = 9.5 \cdot 10^{-3}$  mPa·s if all motors are attached, which is a hundredth of water's viscosity.

### Michaelis-Menten equation

For the stepping rate we use a so-called two-state Michaelis-Menten equation [S1]. The original equation

$$v = C \cdot \Phi \cdot \frac{[S_e]}{[S_e] + k}, \quad (\text{S7})$$

was first introduced by Michaelis and Menten in 1913 to describe enzymatic reaction processes ( $v$ : reaction rate,  $C$  proportionality constant,  $\Phi$ : total molar enzyme concentration,  $[S_e]$ : concentration of free sucrose,  $k$ : dissociation constant which was later on called the *Michaelis-Menten constant*) [S2]. Its shape is characteristic for processes in which reactions are catalyzed by a catalyst  $S_e$  and therefore the associated reaction rates increase with increasing catalyst concentration until it saturates and reaches the value  $C \cdot \Phi$ . In our model we describe the motor stepping rate within this framework, while ATP plays the role of the catalyst. On the one hand we have ATP which is needed to convert the chemical energy in mechanical energy to perform a step, on the other hand we have the force which acts on the motor and reduces its stepping rate. One way to describe these competing counterparts is a coupled Michaelis-Menten equation [S1]

$$s(F_i, [ATP]) = \frac{k_{\text{cat}}(F_i)[ATP]}{[ATP] + k_{\text{cat}}(F_i) \cdot k_{\text{b}}(F_i)^{-1}}, \quad (\text{S8})$$

where  $k_{\text{cat}}$  is the rate constant for the ATP catalysis,  $k_{\text{b}}$  is a second-order rate constant for ATP binding. Both rate constants depend on the load force. As the stepping rate decreases with increasing absolute force  $|F_i|$ ,  $k_{\text{b}}(|F_i|)$  declines faster with force than  $k_{\text{cat}}(|F_i|)$ . Schnitzer *et al.* [S1] introduce a Boltzmann-type force relation for the rate constants

$$k_j(F_i) = \frac{k_j^0}{p_j + q_j \exp(\beta F_i \Delta_j)} \quad j = \{\text{cat}, \text{b}\} \quad (\text{S9})$$

with a constant  $k_j$ ,  $p_j + q_j = 1$ ,  $\beta = (k_{\text{b}}T)^{-1}$  and  $\Delta = \Delta_{\text{cat}} = \Delta_{\text{b}}$  which is the characteristic distance over which the load acts. It was measured for kinesin [S1] and dynein [S3] that the stepping rate, depending on [ATP] and the load force  $F_i$ , can be described by eq. (S8).

It is not conclusively clarified whether the stall force of kinesin and dynein depends on [ATP] or not. Following the experimental results of [S4] we choose dynein's stall



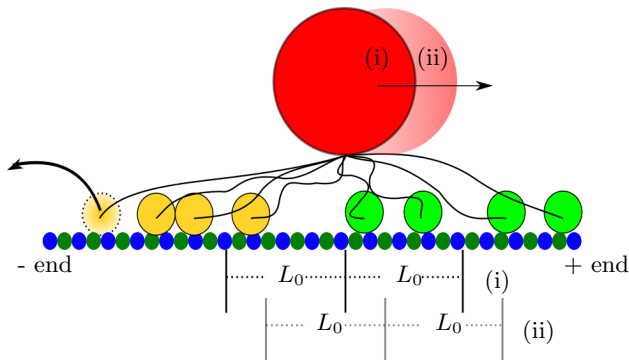


FIG. S1: Sketch of the motor *reservoir*. Assuming that four motors of both kinds are bound to the filament in the given configuration, three minus-end directed motors (yellow) and two plus-end directed motors (green) pull the cargo. If the leftmost motor detaches the cargo will move to the right and therewith also the area of untensioned motors  $x_C(t) \pm L_0$  (going from state (i) to (ii)). In the new motor configuration still three minus-end directed motors and two plus-end directed motors exert a force to the cargo.

force changing with  $[ATP]$  in an affine linear manner from  $F_S([ATP] = 0 \text{ mM}) = 0.3 \text{ pN}$  to  $F_S([ATP] = 1 \text{ mM}) = 1.2 \text{ pN}$  where it saturates, while we leave kinesin's stall force constant at  $2.6 \text{ pN}$ . This determines  $\Delta$  as given in in TABLE S1 to ensure that the stepping rate is zero at stall. We find  $\Delta$  to get  $s(F_S) \ll 1$  by solving the equation

$$\frac{k_{\text{cat}}(F_S)[ATP]}{[ATP] + k_{\text{cat}}(F_S) \cdot k_b(F_S)^{-1}} = 10^{-13} \text{ s}^{-1}, \quad (\text{S10})$$

where we use  $k_{\text{cat}}^0$ ,  $k_b^0$ ,  $q_{\text{cat}}$  and  $q_b$  from Schnitzer *et al.* [S1] and given in TABLE S1..

### Influence of model parameters

In this section we want to analyze the influence of the model parameters on the system's dynamics. We shall now vary one single parameter at a time. The other parameters will keep their value of TABLE S1, while two values for  $[ATP]$  will be considered (0.2 and 1 mM) corresponding to a positive and negative cargo bias, respectively.

First we vary the total number of motors while keeping  $N_+ = N_-$ . We observe that the cargo slows down with increasing motor number and the absolute value of the average bias decreases. One can explain this effect by taking a close look to the motor configuration.

Motors always attach to the microtubule in the force-free area  $x_C(t) \pm L_0$ , and it takes some time before they can apply a force on the cargo. The set of these non-pulling attached motors can be seen as a *reservoir* of motors that can be mobilised very quickly when the config-

uration of pulling motors changes, as illustrated in FIG. S1: when a pulling motor detaches, the cargo moves and new motors from the *reservoir* are involved in the tug-of-war. During this process, the more motors there are in the *reservoir*, the more limited the displacement of the cargo is.

The above argument involves only motors attached to the microtubule. Another way to increase this number is to increase the attachment rate  $k_a$ . Then the bias should decrease. Conversely, increasing the *detachment rate*  $k_d^0$  should lower the number of attached motors and thus increase the bias. This is what is indeed observed in our simulations.

Eventually, if we increase the *force-free velocity*  $v_f$ , the absolute value of the bias increases for both  $[ATP]$  values. Indeed, motors will then exit the force-free area more rapidly, depleting the *reservoir* of non-pulling attached motors.

- 
- [S1] M. J. Schnitzer, K. Visscher, and S. M. Block, *Nature Cell Biology* **2**, 718 (2000).
  - [S2] L. Michaelis and M. L. Menten, *Biochem. z* **49**, 352 (1913).
  - [S3] S. Toba, T. M. Watanabe, L. Yamaguchi-Okimoto, Y. Y. Toyoshima, and H. Higuchi, *Proceedings of the National Academy of Sciences* **103**, 5741 (2006).
  - [S4] R. Mallik and S. P. Gross, *Current Biology* **14**, R971 (2004).
  - [S5] N. J. Carter and R. A. Cross, *Nature* **435**, 308 (2005).
  - [S6] M. A. Welte, S. P. Gross, M. Postner, S. M. Block, and E. F. Wieschaus, *Cell* **92**, 547 (1998).
  - [S7] A. Gennerich, A. P. Carter, S. L. Reck-Peterson, and R. D. Vale, *Cell* **131**, 952 (2007).
  - [S8] A. Kunwar, S. K. Tripathy, J. Xu, M. K. Mattson, P. Anand, R. Sigua, M. Vershinin, R. J. McKenney, C. C. Yu, A. Mogilner, et al., *Proceedings of the National Academy of Sciences* **108**, 18960 (2011).
  - [S9] M. J. I. Müller, S. Klumpp, and R. Lipowsky, *Proceedings of the National Academy of Sciences* **105**, 4609 (2008).
  - [S10] C. Leduc, O. Campàs, K. B. Zeldovich, A. Roux, P. Jolimaitre, L. Bourel-Bonnet, B. Goud, J.-F. Joanny, P. Bassereau, and J. Prost, *Proceedings of the National Academy of Sciences of the United States of America* **101**, 17096 (2004).
  - [S11] R. Mallik, B. C. Carter, S. A. Lex, S. J. King, and S. P. Gross, *Nature* **427**, 649 (2004).
  - [S12] G. T. Shubeita, S. L. Tran, J. Xu, M. Vershinin, S. Cermelli, S. L. Cotton, M. A. Welte, and S. P. Gross, *Cell* **135**, 1098 (2008).
  - [S13] I. M. Kulić and P. C. Nelson, *Europhysics Letters* **81**, 18001 (2008).
  - [S14] A. R. Thiam, R. V. Farese Jr, and T. C. Walther, *Nature Reviews Molecular Cell Biology* **14**, 775 (2013).

|                    | <b>kinesin</b>  | <b>dynein</b>   | Ref.       |
|--------------------|---|---|------------|
| $d$                | 8 nm  |   | [S3, S5]   |
| $N_{\pm}$          | 5   |   | [S6]       |
| $v_f$              | 1000 nm/s   |   | [S3, S5]   |
| $v_b$              | 6 nm/s  |   | [S5, S7]*  |
| $\alpha$           | 0.1 pN/nm   |   | [S8]*      |
| $k_a$              | $5 \text{ s}^{-1}$  |   | [S9, S10]  |
| $k_d^0$            | $5 \text{ s}^{-1}$  |   | [S8]*      |
| $f$                | 1 pN  |   |            |
| $F_S$              | 2.6 pN  | 0.3-1.2 pN  | [S11, S12] |
| $k_d(F)$           | $\begin{cases} k_d^0 \exp\left(\frac{ F }{F_D}\right), & F < F_S \\ k_d^0(1.535 + 0.186 \cdot \frac{ F }{f}), & F \geq F_S \end{cases}$ | $\begin{cases} k_d^0 \exp\left(\frac{ F }{F_D}\right), & F > -F_S \\ k_d^0 \left[ 1.5 \left( 1 - \exp\left(\frac{- F }{1.97f}\right) \right) \right]^{-1}, & F \leq -F_S \end{cases}$ | [S8]*      |
| $k_{\text{cat}}^0$ | $v_f \cdot d^{-1}$  |   | [S1]       |
| $k_b^0$            | $1.3 \mu\text{M}^{-1}\text{s}^{-1}$   |   | [S1]       |
| $q_{\text{cat}}$   | $6.2 \cdot 10^{-3}$   |   | [S1]       |
| $q_b$              | $4 \cdot 10^{-2}$   |   | [S1]       |
| $\Delta$           | 4267.3 nm   | $\max\left(\frac{2.9 \cdot 10^5}{[ATP]^{0.3}} - 28111.1, 8534.6\right)$ nm  | eq. (S10)  |
| Environment        |   |   |            |
| $\eta$             | 100 mPa·s   |   | [S13]*     |
| Cargo              |   |   |            |
| $R$                | 250 nm  |   | [S14]*     |
| $m$                | $5 \cdot 10^{-19}$ kg   |   |            |

TABLE S1: The second and third column show the simulation parameters for kinesin and dynein, respectively. The fourth column gives the references providing experimental basis to these values. The \* indicates that the experimental support gives the order of magnitude only.